MM Science Journal | www.mmscience.eu
ISSN 1803-1269 (Print) | ISSN 1805-0476 (Online)
Special Issue | HSM 2023
17th International Conference on High Speed Machinin
October 25-28, 2023, Nanjing, China
DOI: 10.17973/MMSJ.2023_11_2023103

HSM2023-00010

ANALYSIS OF THIN-WALLED COMPONENTS WITH INTERNAL MICROSTRUCTURE DESIGN MANUFACTURED BY LPBF

M. Martinez-Aguirre[1]*, S. Kumar[2], G. Gómez[1], I. Holgado[3], H. González-Barrio[1], A. Calleja-Ochoa[1], L.N. López de Lacalle[1]

[1]Universidad del País Vasco (UPV/EHU), Department of Mechanical Engineering, Spain

[2]Indian Institute of Technology-Kanpur, Department of Mechanical Engineering, India

[3]Centro de Fabricación Avanzada Aeronáutica (CFAA), Spain

*Corresponding author; e-mail: maialen.martinezdeaguirre@ehu.eus

Abstract
Additive Manufacturing techniques represent a revolution for the design of certain engineering components traditionally subject to a design highly influenced by the manufacturing process linked to the manufacture of the component. Additive Manufacturing techniques therefore allow components with different internal and external structures to be manufactured. Thus, components formed by an internal microstructure are of special interest due to their high strength-to-weight and high stiffness-to-weight properties. This work investigates the hybrid fabrication of curved thin-walled Inconel 718 with internal microstructural supports fabricated by laser powder bed fusion (LPBF). The outer walls are made up of solid surfaces with a fixed curvature and thickness, while the internal structure of the pieces is made up of internal microstructures that vary at different angles of inclination. Finally, the outer surfaces of the piece have been milled. Eventually, the dimensional quality of the components and their internal microstructure has been analysed.

Keywords:
Additive, Microstructure, Inconel, LPBF

1 INTRODUCTION

Superalloys are widely used in aerospace and turbine components. One of the most common is Inconel 718, a precipitation-hardening nickel-chromium alloy which is mainly characterized by its high creep rupture strength, its toughness, and its corrosion resistance at high temperatures. This material consists of two types of strengthening precipitates of the metastable body centred tetragonal γ'' (Ni_3Nb) precipitate and the face centred cubic coherent γ' ($Ni_3(Al,Ti)$) precipitate [Ma 2018]. However, these alloys are difficult to machine due to their low thermal conductivity and diffusivity, which cause steep temperature gradient at the tool edge and the shift the location of the maximum temperature towards the tool tip [Attia 2010].

Compared to conventional subtractive routes, Additive Manufacturing (AM) permits the production of 3D complex near-net-shape components with greatly reduced machining, buy-to-fy ratios close to 1 and shorter production times, while also providing comparable material performances. Among AM techniques, Laser Powder Bed Fusion (LPBF) consists of a layer-by-layer selective melt of a powder bed using a focused energy source.[Serrano 2020]. Moreover, the melt pool in LPBF can be identified with a high thermal gradient and rapid cooling rate (~10^6 K/s) up to ambient temperature; thus, elemental segregation is greatly suppressed while an increase in dislocations is favoured [Gokcekaya 2021].

Laser Powder Bed Fusion technique is becoming an attractive and promising process to treat Inconel 718 for the fabrication of complex components with high dimensional accuracy and with good surface integrity in some industries. In particular, it is been applied in aerospace machine shafs bearings, and jet engine turbines due to its strong thermal resistance, high micro-hardness and strength, and excellent fatigue deformation resistance at high temperature. [Kim 2017].

The responsibility of aerospace industries, subsequently of researchers in the manufacturing industry, is to devise a sustainable strategy focused on reducing the global warning. Notwithstanding the fact that the sustainable production of nickel-based alloys remains a challenge for the manufacturing industry, recent researches have helped to fill this quantitative knowledge gap, analysing the cradle-to-gate energy and GHG emission footprints of lightweight aircraft components [Huang 2016] and evaluating the

sustainability of Inconel 718 in Laser Powder Bed Fusion (LPBF) processes [Gruber 2021].

Previous work was performed by the authors about the influence of LPBF process in the final component mechanical properties made by Inconel 718. It was observed that the process definition along with the design of the layer formation can affect to the static and dynamic stiffness and damping. Therefore, LPBF process presents the advantage of flexibility and complex geometries formation that absorbs vibration during the final machining obtaining a more rigid part [Perez 2023].

The present study investigates the hybrid manufacturing of Inconel 718 curved thin walls with internal microstructural supports fabricated by LPBF. Thus, this small-scale curved component supported by internal microstructure is designed analogously to static shell components. Afterwards, the limiting size of the internal microstructure (<200 *μm*) is checked for Inconel 718 LPBF. These microstructures are used to support thin walls in different orientations from the wall surface.

Moreover, an LPBF solid thin wall with no internal microstructure is printed, in order to compare the geometrical accuracy with the curved thin-walled with different microstructure orientations (60º, 90º and 120º). To conclude the process, finish milling of the printed parts is performed as a means to analyse the geometrical accuracy before and after milling.

2 DESIGN SPECIFICATIONS

Through the Siemens NX Software, four thin-walled pieces are modelled with different internal microstructure orientation.

The piece number one is solid and does not have internal microstructure, the second one's microstructure has an inclination of 120 degrees, the third one's orientations is of 90 degrees and the fourth one's of 60 degrees. These pieces are placed on the construction platform for the manufacturing process as shown in Fig. 1.

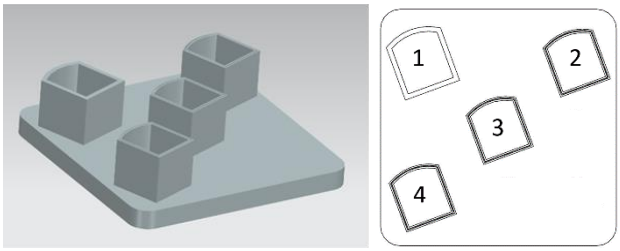

Fig. 1: Thin-walled pieces CAD design and distribution.

The outer and inner surfaces of all the pieces are patterned with the same dimensions as are presented in Figure 2. The solid piece does not have microstructure, but the orientation of the microstructure of the pieces 2, 3 and 4 is also shown in Fig. 2.

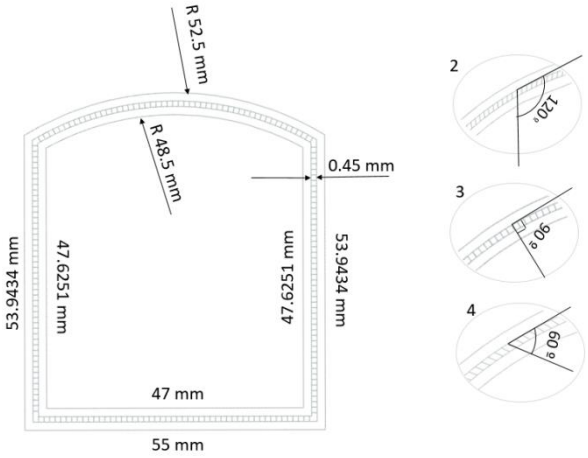

Fig. 2: Dimensions and microstructure orientation of pieces 2, 3 and 4.

2.1 Material

Inconel 718 powder with the nominal size of 17.1 *μm*, 32.6 *μm* and 54.8 *μm* is used as the raw material for the curved thin walls. Gas atomized IN718 powder is composed of nickel (Ni), chromium (Cr), iron (Fe), niobium (Nb), molybdenum (Mo) and other elements in traces. The chemical composition of IN718 is given Tab. 1.

Tab. 1: *Chemical composition of IN 718.*

Element	Ni	Cr	Fe	Nb	Mo
wt.%	54.14	18.4	17.42	4.85	3.03

3 MANUFACTURING PROCESS

The designed four thin-walled pieces are printed with the Additive Manufacturing process LPBF because of its high dimensional accuracy.

Laser Powder Bed Fusion processing parameters for different features of the printed parts are shown in Tab. 2.

Tab. 2: LPBF processing parameters.

Parameters	Thin walls	Internal microstructure
Laser power (W)	200	124
Scan strategy	Stripe	Single line
Exposure time (*μs*)	80	40
Point distance (*μm*)	70	20
Hatch distance (*μm*)	90	-
Layer thickness (*μm*)	60	60

These printed pieces are solution annealed at 954 degrees by an hour. Then, they are quenched and precipitated at 718 degrees for 8 hours. Afterwards, the pieces are furnace cooled at 621 degrees for 8 hours and 49 minutes and finally, they are held for 1 hour and 11 minutes. It is vital to stress that all these processes are carried out before the milling process.

The outer surfaces of the printed pieces are milled (Fig. 3) in Kondia A6 with WC/Co end mills (3 flutes, diameter of 8 millimetres, helix angle 42 degrees, fine grade carbine, Mikron tools – Germany) under cooling environment in order to reduce any adverse thermal influence.

These milling parameters are presented in Tab. 3.

Tab. 3: Milling parameters.

Parameters	Value
Milling speed (m/min)	80
Feed (mm/rev)	0.02
Axial depth of cut (mm)	2
Radial depth of cut (mm)	0.5

Fig. 3: Outer surfaces finish milling.

Finally, a Coordinate Measuring Machine (CMM-Zeiss MC80-Germany) with a 3-millimetre diameter ceramic stylus is used for achieving an accurate measurement for the dimensional analysis as it is shown in Fig. 4.

Fig. 4: CMM-Zeiss MC80-Germany.

Moreover, in order to complete this study, a tomography analysis is performed to evaluate the manufacturing process and to check if the internal channels are correctly manufactured maintaining the geometry in dimension and angle.

In this present study, X-ray Computed Tomography (CT) is used to analyse geometrical deviations of the samples. CT is a non-destructive testing technique that can provide unrivalled information about the internal structure of Additive Manufacturing parts.

During a CT scan, a sequence of radiographs (two-dimensional images) are taken from a number of different directions of a complete revolution of the sample using the penetrating power of X-rays radiation. Afterwards, a computed reconstruction algorithm is used to obtain a 3D digital representation of the scanned sample.

CT datasets are acquired by a General Electric X-Cube Compact machine, by a cone beam system with a stationary X-ray tube and flat panel detector. During CT scans, the voltage is set to 192 kV whereas the tube current is adjusted to be high enough to minimize the exposure. Thus, the tube current is adjusted to 2,7 mA and the exposure time to 70 ms. In addition, beam hardening is reduced by combining 1 mm copper and 0.5 mm tin filters. The samples are placed into the machine as shown in the Fig. 5 and the resulting voxel size is 95µm^3. Geometrical deviations in the reconstructed scan data are analysed with the Volume Graphics VGStudio Max 3.4 software.

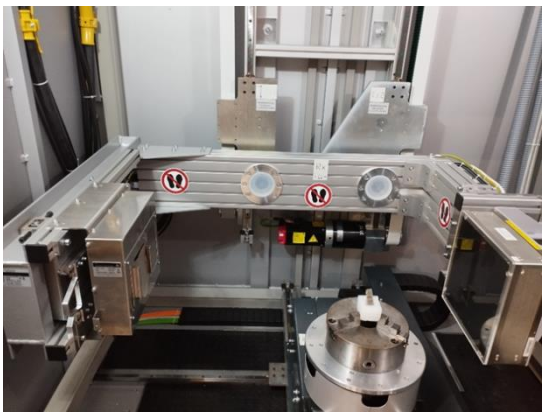

Fig. 5: General Electric X-Cube Compact machine.

4 RESULTS

4.1 CMM measurement

According to the Coordinate Measuring Machine, it can be appreciated that no noticeable damage has occurred to the microstructures. Nevertheless, some of the microstructures are filled with chip fragments and burrs because of the available space in the microstructured parts. In spite of this, the crucial point is that there have been no ruptures, fractures or detachments of the internal or external walls.

Another noteworthy outcome measured with this machine, is that the measured external diameter of the finished part deviates from the theoretical diameter after milling, as it is presented in Fig. 6. This image shows the theoretical outer diameter of each piece (TD) which is represented in yellow. Moreover, each part is analysed before machining (NM), presented in blue, and after machining (M), presented in grey. The legend of the graph represented in Fig. 6 is shown in Tab 4.

Tab. 4: Legend of Fig. 6.

Piece	NMC (Not Machined Curved piece)	MC (Machined Curved piece
1(solid)	NMC1	MC1
2(120º)	NMC2	MC2
3(90º)	NMC3	MC3
4(60º)	NMC4	MC4

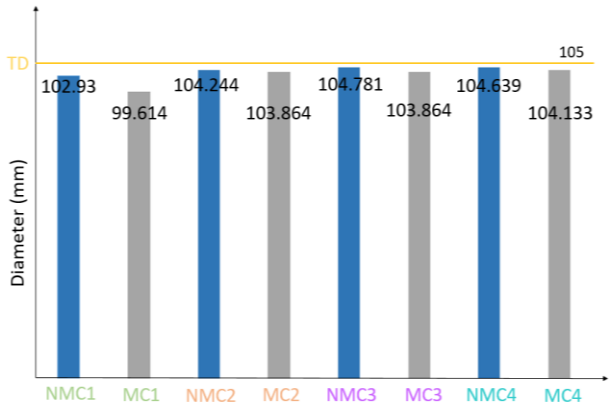

Fig. 6: Comparison between the theoretical and real diameter.

Therefore, it is experimentally proposed that 60° microstructure orientation is the best after machining, and as it was evident, it is demonstrated that the diameter of the parts after machining decreases.

Furthermore, not only de diameter of the finished part have been measured, but also the parallelism and perpendicularity. These measurements of the fourth pieces before and after milling are presented in Fig. 7. It was observed that there is a high variability from non-machined and machined parts, this stems from the process per se. The LPBF process offers near-net-shape geometries, however depending on the design there are big differences observed in figure 7. These differences could be a non-welded particles or pores formation. Machined components prove that post-processing is needed in order to achieve final component specifications, particularly in thin walls, to ensure surface quality and integrity.

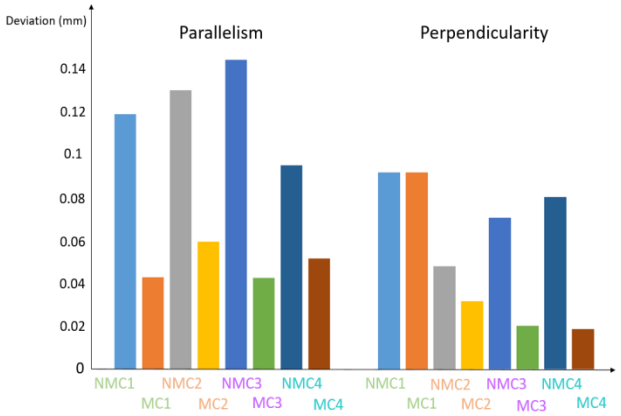

Fig. 7: Parallelism and perpendicularity before and after machining.

Some reasons for pieces diametric deviations can be considered to be residual stresses in printed parts, compression induced by machining on the outer wall, compression and plastic deformation of internal microstructures (administered between inner and outer walls), and measurement error caused by selection of local points along the length (axis) of the cylindrical walls or measurement errors.

4.2 Tomography with X-rays measurement

Computed Tomography takes a sequence of radiographs from different directions of a complete revolution using the penetrating power of X-ray radiation, and then uses a computer reconstruction algorithm to obtain a 3D digital representation of the scanned specimen. Using advanced analysis software, the 3D model can be further analysed both qualitatively and quantitatively.

After the tomographic analysis, it can be appreciated that there is a lack of penetration in the corners of the pieces as it is shown in Fig. 8. Therefore, there is no efficient determination in these regions of the tomography and the channels are not reproduced there.

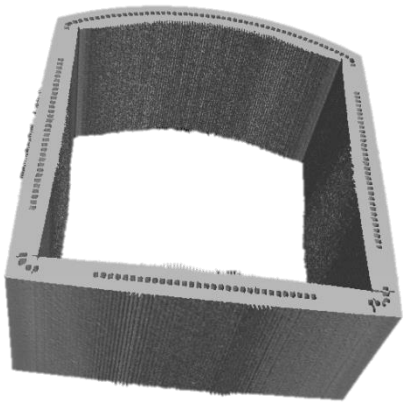

Fig. 8: Tomography section.

The present study investigates five channels (the number of channels analysed is set to five so that the study does not take a great deal of time) in order to evaluate the manufacturing process, which are selected due to their higher TC quality.

These channels are used for the determination of geometrical measurements. For instance, walls angles and minimum distance between two walls are measured.

The angle of each wall is obtained between two geometric elements. The first one is a plane named as "Element 1" and it is shown in Fig.9. This element is the machined area, the flattest surface, and is adjusted by least squares with a high density of points (>10,000).

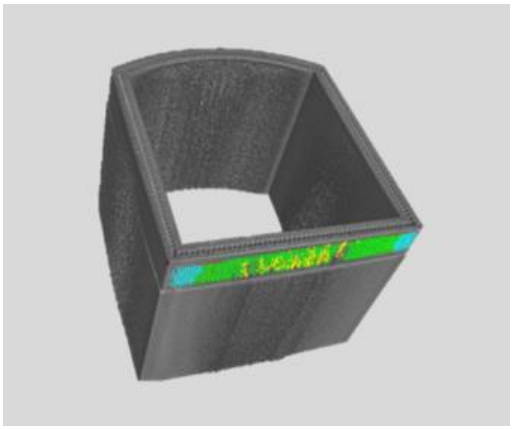

Fig. 9: Element 1

According to the second element, "Element 2", it is composed by a group of planes, 12 channel walls, presented in Fig. 10, and each channel wall is evaluated by fitting planes in the same way by least squares with a high density of points (>10,000).

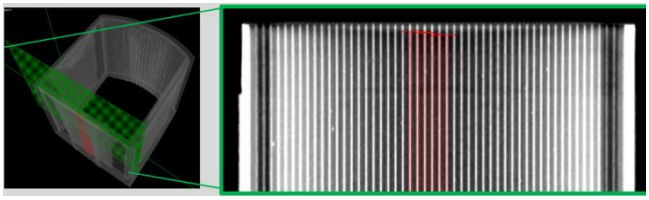

Fig. 10: Element 2.

Each channel wall is listed as defined in Fig. 11.

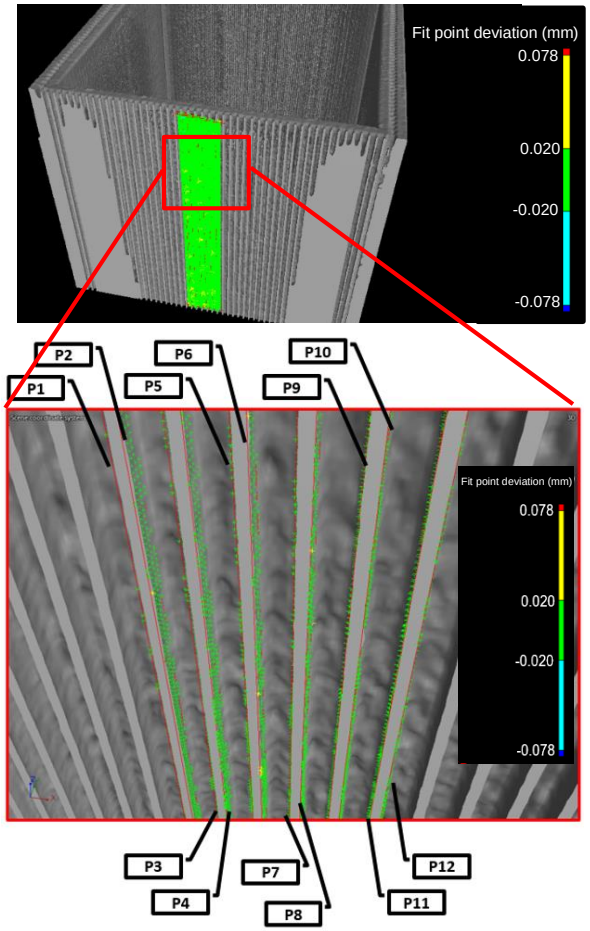

Fig. 11: Channel walls distribution.

The reported distance between walls is obtained by the minimum distance (orthogonal to the adjacent element on the left) between the two geometric elements. In Fig. 12, the example of the measurement of minimum distance between P1 and P2 is shown.

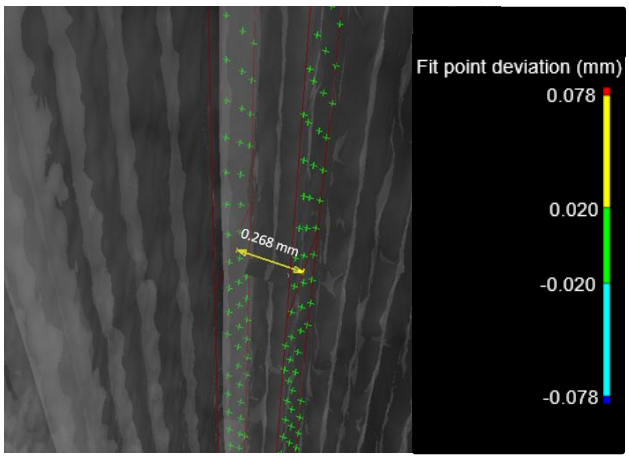

Fig. 11: Measurement of minimum distance P1-P2.

In the Tab. 5, the measurements obtained from this process compared with the nominal distance are collected. It can be appreciated that the maximum real distance compared with the nominal one is of 75 *μm,* whereas the minimum real distance compared with the nominal distance is of 68 *μm.* Besides that, it is also worth mentioning that the real distance is in all cases bigger than the nominal one. This could be because of the lack of thermal softening in the flood cooling method.

Tab. 5: Minimum distance between walls.

Elements	Nominal distance (mm)	Real distance (mm)
P1-P2	0.200	0.268
P3-P4	0.200	0.272
P5-P6	0.200	0.275
P7-P8	0.200	0.274
P9-P10	0.200	0.271
P11-P12	0.200	0.269

In addition, the angle of each wall is measured orthogonally as it is presented in Fig. 13, the example of the angle measurement of P2 wall.

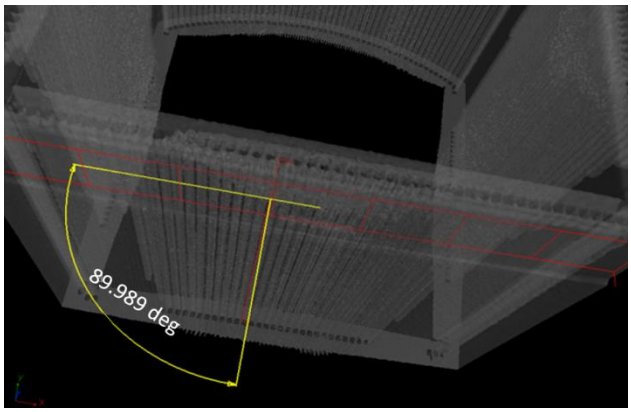

Fig. 12: Angle measurement of P2.

In the Tab. 6, the measurements of each walls angles compared with the nominal angles are collected.

Tab. 6: Comparison between nominal and real angles.

Element	Nominal angle (°)	Real angle (°)

P1	90	88.851
P2	90	89.989
P3	90	90.308
P4	90	88.851
P5	90	89.807
P6	90	88.518
P7	90	90.837
P8	90	88.687
P9	90	90.494
P10	90	88.864
P11	90	90.731
P12	90	89.021

As can be clearly noticed in Fig. 14, the measured angles of the finished part deviate from the theoretical ones. Some of them increase, while most of them decrease. However, taking into consideration the angle that increased the most, P7, has increased 0.837 degrees, whereas the one that has suffered the biggest geometric reduction, P6, has decreased 1.482 degrees.

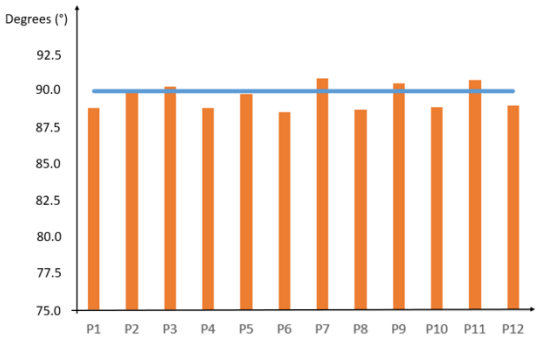

Fig. 13: Comparison between nominal and real angles.

5 CONCLUSIONS

In this present study, the hybrid manufacturing strategy for lightweight Inconel 718 components is presented, so that an interesting approach to develop lightweight IN718 printed parts using the Laser Powder Bed Fusion process is shown and the influence of microstructure-support orientations on the finish milling operation is analysed. According to the coordinate measurement with the CMM and the tomography with the X-Rays measurement, the following conclusions are compiled:

- All four parts have been printed without any geometric distortion, and the internal microstructures have not suffered any damage either.
- It is also essential to note that no breakage, spalling or fractured supports were noticed after finish milling, therefore, the milling process does not damage the integrity of the internal microstructure supports.
- However, some diametrical deviations have been identified. One possible explanation could be the residual stresses of superalloy components due to the fact that they affect the accuracy of the finished components. Furthermore, the measurement of residual stresses and their impact on the geometric deflection of the components is beyond the scope of the present study.
- On contrary, the repeatability of the measurements has been guaranteed by calibrating the CMM with the standards supplied, so it could not have altered the results obtained.
- Meanwhile, it has to be mentioned that the piece with 120 degrees microstructure orientation is the closest to the theoretical dimensions.
- In terms of future lines of research, on the one hand, with regard to the CMM measurement, it would be interesting to carry out a more exhaustive study in finding the reason why there has not been sufficient penetration, since it was programmed in the design. On the other hand, as for the tomographic measurement, it would be interesting to carry out a complete measurement of all the channels instead of focusing only on five channels. This process was no feasible in this study due to the fact that it would take unreasonably long times.

6 REFERENCES

[Attia 2010] Attia, H., et al. Laser-assisted high-speed finish turning of superalloy Inconel 718 under dry conditions. CIRP Annals, 2010, Vol.59, No.1, pp. 83-88.

https://doi.org/10.1016/j.cirp.2010.03.093

[Gokcekaya 2021] Gokcekaya, O. et al. Unique crystallographic texture formation in Inconel 718 by laser powder bed fusion and its effect on mechanical anisotropy. Acta Materialia, Vol. 212, 2021, pp.116876-116887

https://doi.org/10.1016/j.actamat.2021.116876

[Gruber 2021] Gruber, K., et al. Evaluation of Inconel 718 Metallic Powder to Optimize the Reuse of Powder and to Improve the Performance and Sustainability of the Laser Powder Bed Fusion (LPBF) Process, Materials, 2021, Vol. 14, No. 6, pp.1538-1565.

https://doi.org/10.3390/ma14061538

[Huang 2016] Huang, R., et al. Energy and emissions saving potential of additive manufacturing: the case of lightweight aircraft components. Journal of Cleaner Production, 2016, Vol. 135, pp. 1559-1570.

https://doi.org/10.1016/j.jclepro.2015.04.109

[Kim 2017] Kim, S. et al. Thermo-mechanical improvement of Inconel 718 using ex situ boron nitride-reinforced composites processed by laser powder bed fusion. Scientific Reports, 2017, Vol.7, No1.

https://doi.org/10.1038/s41598-017-14713-1

[Ma 2018] Ma, S., et al. Effects of temperature on microstructure and mechanical properties of IN718 reinforced by reduced graphene oxide through spark plasma sintering. Journal of Alloys and Compounds, 2018, Vol. 767, pp. 675-681.

https://doi.org/10.1016/j.jallcom.2018.07.071

[Perez 2023] Pérez-Ruiz, J.D., et al. Machining stability Improvement in LPBF printed components through stiffening by crystallographic texture control. CIRP Annals.

https://doi.org/10.1016/j.cirp.2023.02.025

[Serrano 2020] Serran, I., et al. The residual stress in as-built Laser Powder Bed Fusion IN718 alloy as a consequence of the scanning strategy induced microstructure, Scientific Reports, 2020, Vol.10, No.1.

https://doi.org/10.1038/s41598-020-71112-9